Sensors and Actuators B 174 (2012) 87–93

Contents lists available at SciVerse ScienceDirect

Sensors and Actuators B: Chemical

journal homepage: www.elsevier.com/locate/snb

Functionalization layers for CO_2 sensing using capacitive micromachined ultrasonic transducers

Hyunjoo J. Lee[a,*], Kwan Kyu Park[a], Mario Kupnik[b], Butrus T. Khuri-Yakub[a]

[a] Edward L. Ginzton Laboratory, Center for Nanoscale Science and Engineering, Stanford University, Stanford, CA 94305, USA
[b] Brandenburg University of Technology, 03046 Cottbus, Germany

ARTICLE INFO

Article history:
Received 1 June 2012
Received in revised form 10 August 2012
Accepted 13 August 2012
Available online 23 August 2012

Keywords:
CO_2 detection
CMUT
Resonant chemical sensor
CO_2 polymers

ABSTRACT

Sensing of carbon dioxide (CO_2) using inexpensive, miniaturized, and highly sensitive sensors is of great interest for environmental and consumer applications. In this paper, we present four functionalization layers that are suitable for resonant sensors based on mass-loading for CO_2 detection. We compare the volume sensitivities of these layers to CO_2 and relative humidity (RH) by using a highly sensitive 50-MHz capacitive micromachined ultrasonic transducer (CMUT) as a resonant sensor. Among the four functionalization layers, the layer based on a guanidine polymer exhibits the highest volume sensitivity to CO_2 of 1.0 ppm/Hz in N_2 and 3.8 ppm/Hz in air (~45%RH). Furthermore, we report on other important characteristics of the guanidine polymer for sensing applications, including polymer saturation, regeneration, and repeatability.

1. Introduction

The demand for carbon dioxide (CO_2) sensors is high because of their potential uses in a broad range of applications, including consumer, industrial, and agricultural applications. For example, CO_2 sensors play an important role in monitoring and controlling indoor air quality. When the level of CO_2 is elevated above 1000 ppm from the level in fresh air (~300 ppm) due to, for example, inadequate ventilation, approximately 20% of occupants in the room begin to feel discomfort. CO_2 sensors are also critical in the food processing industry; controlling the CO_2 level inside the storage packaging is essential to maintaining the freshness and shelf life of food. Other places that benefit from CO_2 sensors include breath analyzers in healthcare, environmental incubators in biotechnology and petrochemical plants in industry.

The great number of potential applications has been an impetus for the developments of miniaturized CO_2 sensors based on microtechnology. Compared to existing CO_2 sensing systems based on infrared spectroscopy or gas chromatography, the miniaturized CO_2 sensors are attractive because of their small size, low cost, low power consumption, and CMOS compatibility. Among miniaturized sensors, resonant chemical sensors based on the mass-loading mechanism offer competitive advantages, such as superior sensitivity, high resolution, and a wide dynamic range [1]. Thus, by applying a chemically sensitive layer to the resonant structures, many resonant devices have been developed as chemical sensors. Examples are micro/nano-cantilevers [2], quartz crystal microbalance (QCM) devices [3], surface acoustic wave (SAW) devices [4], and capacitive micromachined ultrasound transducers (CMUTs) [5].

Developing a resonant sensor for CO_2 detection, however, is challenging because it is difficult to find a functionalization layer that would be both sensitive and selective to CO_2 at room temperature. The layers that are chemically sensitive to CO_2 have previously been explored and developed for various applications, such as sensing, separation, and capture of CO_2. These layers include metal-oxide thin-films [6], layers that are functionalized with amino-groups [7], carbon nanotubes [8], and synthesized polyimide films [4]. Metal-oxide thin-films react with CO_2 only at elevated temperatures (~300–400 °C) and other functionalization layers lack the chemical sensitivity or resolution to be used at ambient conditions (Table 1). In addition, a functionalization layer sensitive to CO_2 is often also sensitive to H_2O, and, thus, the cross-sensitivity to H_2O must be characterized.

This paper first presents a comparative study on the volume sensitivities of the CMUTs to CO_2 and H_2O which are coated with various functionalization layers suitable for a resonant sensor system based on the mass-loading mechanism. (Volume sensitivity in this work is defined as the sensitivity to the gas concentration expressed as a volume fraction.) CMUTs operating at a mechanical resonant frequency of 50 MHz are chosen as the sensing platforms because of their superior sensitivity with a mass resolution below 1 ag (10^{-18} g), inherent array structure, and low thermal noise due to massive parallelism [5]. Among the various functionalization layers used in this work, the guanidine polymer exhibited the best

* Corresponding author. Tel.: +1 650 644 5800; fax: +1 650 725 3890.
E-mail address: hyunjoojlee@gmail.com (H.J. Lee).

0925-4005/$ – see front matter © 2012 Elsevier B.V. All rights reserved.
http://dx.doi.org/10.1016/j.snb.2012.08.025

Table 1
Comparison of highly sensitive resonant chemical sensors based on mass-loading for CO_2 detection.

Resonant device	Layers	Sensitivity (ppm/Hz)	Resolution[a] (ppm)
SAW [4]	Homo-polyimide	13.8	820
Resonant MEMS sensor [8]	Carbon nanotubes	104	7000
QCM [3]	APTMS/PTMS[b]	8.3[c]	50
CMUT (this work)	Guanidine	1.05	4.9

[a] 1-σ confidence level.
[b] APTMS: (3-aminopropyl)-trimethoxysilane; PTMS: propyltrimethoxysilane.
[c] Operating temperature: 70 °C.

sensitivity of 3.8 ppm/Hz and a resolution of 17.7 ppm (1σ) to CO_2 at ambient condition (~45%RH). Considering that the CO_2 concentration at ambient condition is 300 ppm (0.03%) and the threshold limit value (TLV) for CO_2 is 5000 ppm (0.5%), our sensor provides more than sufficient sensitivity and resolution. Thus, we further investigated the characteristics of the sensor functionalized with the guanidine polymer including polymer saturation and regeneration, sensor repeatability, and cross-sensitivity to water vapor.

2. Methods

2.1. CMUT sensor system

A CMUT-based sensor system, operating at a mechanical resonant frequency of 50 MHz, is used to investigate the sensitivity of various functionalization layers for CO_2 detection. The operational principle of the CMUT resonant sensor is mass-loading; an increase in the mass of the resonant structure results in a decrease in the resonant frequency, as estimated by the following equation:

$$\Delta f_0 = -\frac{1}{2} \times \frac{f_0}{m} \times \Delta m, \quad (1)$$

Using the mechanical resonant frequency, f_0, of approximately 50 MHz and an effective mass of the resonant plate of 103 pg, our CMUT resonant sensor achieves an excellent mass sensitivity of 4.3 ag/Hz (or 49 zg/Hz/μm^2). The surface of this highly sensitive mass sensor is modified by a chemically sensitive layer to be specific and sensitive to the analyte of interest. Physisorption or chemisorption of the analyte molecules on the sensitive layer increases the mass, which results in a decrease in the resonant frequency proportional to the mass change.

A single CMUT resonant sensor consists of hundreds to thousands of identical circular capacitive resonators, packed for example in a hexagonal-shaped arrangement (Fig. 1(a)). These individual resonators are all electrically connected in parallel through the common top electrode to form a multi-resonator configuration. A multi-resonator configuration offers the benefit of signals with reduced thermal noise, which determines the limit of detection (LOD), i.e. the resolution of the sensor system [9]. Twenty-two of these CMUT resonant sensors are placed in an array structure on a 2.5-mm-by-5-mm die to allow multichannel detection (Fig. 1(b)). These sensors share the electrical ground connection through a heavily doped silicon substrate.

The basic resonant structure of the 50-MHz CMUT is a parallel-plate capacitor with a circular plate with a radius of 5.3 μm (Fig. 2). The top electrode is a 500-nm thick heavily doped single-crystal silicon plate, while the bottom electrode is the electrically conductive silicon substrate. These two electrodes are separated by a 50-nm vacuum cavity. The top plate is supported by a 1-μm thick thermally grown silicon dioxide post [10]. The first flexural-mode (0,1) resonant frequency for a circular plate is given by [11]

$$f_0 = \frac{0.83}{a}\sqrt{\frac{Et^3}{m(1-\nu^2)}}, \quad (2)$$

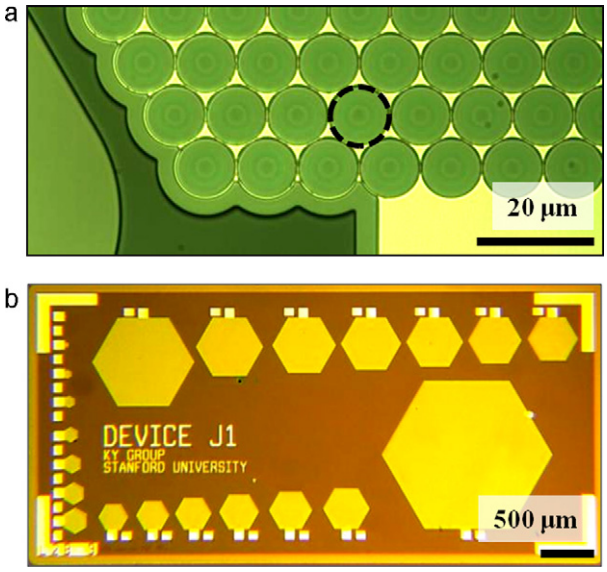

Fig. 1. Top-view optical pictures of (a) a section of a single sensor, showing multiple circular resonant structures connected in parallel to form a single device, and (b) a die showing an array of multiple sensors.

where a is the radius, E is the Young's modulus, t is the thickness, ν is the Poisson ratio, and m is the mass of the circular plate. By designing for a small radius and using single-crystal silicon with a small equivalent mass for the plate, we achieved a CMUT resonant sensor with a high mechanical resonant frequency of approximately 50 MHz.

The electrical input impedance of a CMUT sensor biased at various DC voltages was measured by using an impedance analyzer (Agilent Technologies, Model 4294A, Palo Alto, CA) to examine the resonant characteristics. The AC amplitude of the source of the impedance analyzer was set to 50 mV_{RMS}. The CMUT sensor, consisting of 1141 resonators, biased at 48 V exhibits a series resonant frequency of 43.0 MHz and a parallel resonant frequency of 44.6 MHz (Fig. 3). The input impedance data was then fitted to the conventional Butterworth van Dyke (BvD) model to provide an

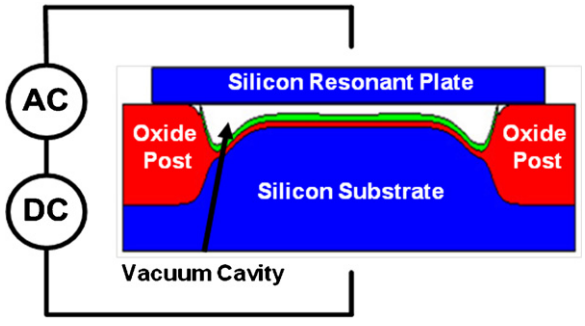

Fig. 2. Schematic cross-sectional view of a single circular CMUT resonator.

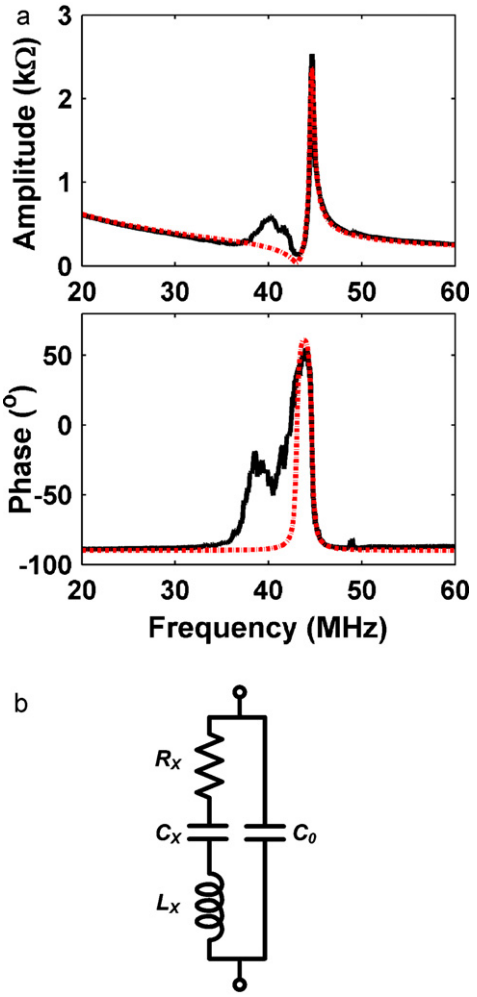

Fig. 3. (a) Plot of measured and fitted (dotted line) input impedance characteristics of the CMUT resonator biased at 48 V ± 50 mV_{RMS}, in air. (b) Schematic of 4-element van Dyke equivalent circuit model used to fit the input impedance data of the CMUT.

equivalent circuit model for the interface circuit design [12]. The model fails to accurately predict the impedance near the series resonant frequency because the BvD model assumes a single resonator structure with equal quality factors (Q) at both resonances. Due to the massive parallelism of the CMUT structure, Q at the series resonant frequency (Q_s = 44) is much smaller than that at the parallel resonant frequency (Q_p = 120). Thus, we designed an opamp-based oscillator to track the parallel resonant frequency using the equivalent circuit model and implemented it on a printed circuit board (PCB) using off-the-shelf discrete components [5].

2.2. Functionalization layers

We examined four functionalization layers in terms of their sensitivity to CO_2 and reversibility by applying them on top of the CMUT (Table 2). The added mass from the functionalization layer was insignificant to affect the mass sensitivity of the device because the densities and thicknesses of functionalization layers are much smaller than that of the silicon resonant plate. These layers can be categorized into two types according to their interactions with CO_2. The first type (Type I) reacts directly with CO_2 through acid base interaction and includes, for example, polymers that are functionalized with a highly basic amine group. The second type (Type II) is the one that has a high solubility to CO_2, such as polyimides developed for membrane separation of CO_2.

The first Type I material investigated is an organically modified silicate functionalized with primary amine-group, (3-aminopropyl)-trimethoxysilane (APTMS), which was co-condensed with propyltrimethoxysilane (PTMS) in 1:3 ratio [13]. The second material examined is polyhexamethylene biguanide (PHMB), a member of guanidine polymer family, which has basic amide-bearing functional groups. In addition, a non-polymeric Type I material, a mesoporous silica layer functionalized with a primary amine-group, (3-aminopropyl)-triethoxysilane (APTES) is also investigated [7]. The material tested for Type II is a glassy polymer with a high solubility, a homopolyimide developed by Hoyt et al. This homopolyimide is a mixture of hexafluoroisopropylidene diphthalic anhydride (6FDA) and 2,3,5,6-tetramethyl-1,4-phenylenediamine (4MPD) [4].

Prior to the functionalization, the CMUT devices were first pre-cleaned in acetone, methanol, and isopropanol and dried using a nitrogen gun. The functionalization layers were then applied using various coating methods, such as spin-coating and dip-coating, and the thicknesses of the layers were estimated using the tools specified in Table 2. For APTMS/PTMS, the mixture was poured over the sensor, removed by running it off the edge of the device and incubated in a humidity chamber for 30 min. All the chemicals were used as received without further purification from Sigma–Aldrich (St. Louis, MO, USA), Arch Chemicals, Inc. (Norwalk, CT, USA), Ashland, Inc. (Covington, KY, USA) and Adherent Technologies, Inc. (Albuquerque, NM, USA).

2.3. Experimental system

The CMUT were interfaced with free-running oscillators tracking the changes in the resonant frequencies in real-time. The output of the oscillator was connected to a frequency counter (Stanford Research Systems, Model SRS620, Sunnyvale, CA) and the measured frequency data was transferred to a regular personal computer via General Purpose Interface Bus (GPIB). We evaluated the volume sensitivity of a CMUT sensor by exposing the sensors, enclosed in a glass chamber (0.8 cm^3), to various controlled concentrations of CO_2 and H_2O in N_2. We generated various concentrations of analytes by using mass flow controllers to adjust the flow rate of the analyte and the carrier gas (N_2). In addition, the saturation bubbler method [5] was used to generate H_2O vapor.

Another important parameter of our sensor system is the resolution or LOD, which indicates the smallest concentration the sensor can detect. In a resonant sensor system, the LOD is determined by the system frequency noise (δf) in Hz and the volume sensitivity in ppm/Hz. In this work, we used an overlapped Allan deviation, which is a common measure of short-term frequency stability in the time-domain. It is defined as [14]:

$$\sigma_y(\tau) = \sqrt{\frac{1}{2(M-1)}\sum_{i=1}^{M-1}(y_{i+1}-y_i)^2}. \quad (3)$$

where M is the number of frequency samples and y is the fractional frequency. The fractional frequency, $y(t)$, is defined as the ratio of a difference in the oscillation frequencies, $f(t)-f_0$, to the nominal oscillation frequency, f_0, at the given sampling time. First, successive frequency samples without dead-time were recorded over a sampling period at a fixed sampling time. Square roots of two-sample variances were then computed on this data for different sampling times to find the minimum variance.

Table 2
Summary of the functionalization layers investigated in the comparative study.

Functionalization layer	Abbreviation	Reaction type	Coating method	Coating parameters
APTMS:PTMS (1:3)	APTMS/PTMS	Type I	Rinsing	Solvent: none Iteration: once Thickness: ~70 nm (Profilometer)
APTES-functionalized mesoporous layer	APTES	Type I	Dip coating	Solvent: ethanol Pull-out speed: 6 mm/min Thickness: 85 nm (SEM[a])
6FDA:4MPD	Homopolyimide	Type II	Spin coating	Solvent: chloroform Spin-speed: 3 krpm Thickness: 55 nm (Ellipsometer)
PHMB (20%)	Guanidine	Type I	Spin coating	Solvent: 1:1 IPA:water Spin-speed: 2 krpm Thickness: 70 nm (Profilometer)

IPA: isopropyl alcohol.
[a] SEM: scanning electron microscope.

3. Results and discussion

3.1. Comparative study on CO_2 sensitivity

The CMUT functionalized with four different layers were exposed to various concentrations of CO_2 in dry N_2 from 0 ppm to 20,000 ppm (i.e. from 0% to 2%). As predicted, the oscillation frequencies of the CMUT decreased when the functionalization layers reacted with CO_2 and increased back to the baseline when the chamber was purged with the carrier gas (Fig. 4). The sensors were characterized at room temperature, except for the one functionalized with APTMS:PTMS. APTMS reacts with CO_2 in the presence of water as described in

$$Si(OCH_3)_3(CH_2)_3NH_2 + H_2O + CO_2 \rightleftharpoons Si(OCH_3)_3(CH_2)_3NH_2^+HCO_3^-,$$

where the equilibrium of the reaction is on the right-hand side below 60 °C indicating a slow desorption of CO_2 at room temperature [13]. As the equilibrium lies far to the right-hand side at room temperature, the as-deposited APTMS:PTMS layer (left in ambient over 2 weeks prior to the chemical test) would absorb CO_2 from air. Desorption of CO_2 from the as-deposited layer through purging with N_2 can be accelerated by increasing the operating temperature. Therefore, the APTMS:PTMS sensor unit was evaluated at an elevated temperature of 60 °C.

The maximum frequency shifts at different CO_2 concentrations are used to compute the volume sensitivity of each sensor (Fig. 5). The volume sensitivity of each sensor is estimated by first computing the slope using the best-fit linear regression and then taking the inverse of the slope. For the CMUT functionalized with guanidine, the maximum frequency shifts continued to increase as the CO_2 concentration increased. However, this happened at a smaller increment due to polymer saturation. Thus, we used a best-fit linear regression at the linear regime between 0 ppm and 12,000 ppm (i.e.

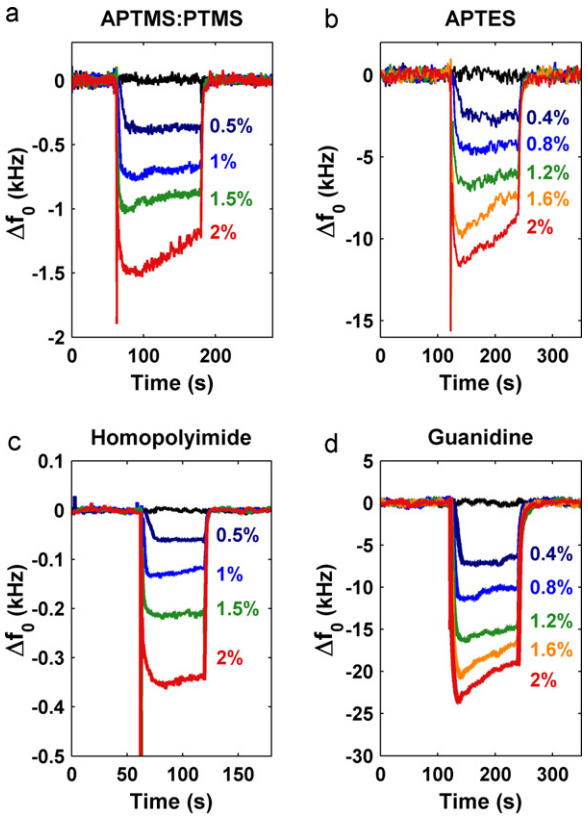

Fig. 4. Transient frequency shifts in response to various concentrations of CO_2 in N_2 of the CMUT sensors functionalized with (a) APTMS:PTMS, (b) APTES, (c) homopolyimides, and (d) guanidine. CO_2 starts to flow in at 60 s or 120 s and stops at 240 s or 360 s, respectively. The CO_2 concentrations are represented in % where 1% is equivalent to 10,000 ppm.

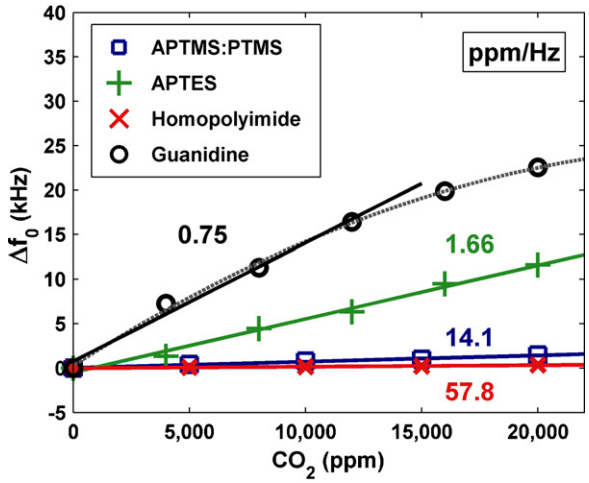

Fig. 5. Plot of maximum frequency shifts observed at different CO_2 concentrations in N_2 for four sensors. The numbers indicate the volume sensitivities in ppm/Hz which were estimated using the best-fit linear regression.

Table 3
Summary of volume sensitivities and resolutions of the CMUT sensors to a small range of CO_2 concentrations (0–20,000 ppm) and a wide range of H_2O concentrations (0–100%RH), in N_2.

Layers	Frequency noise (Hz) (1σ)	CO_2			H_2O		
		Sensitivity (ppm/Hz)	Resolution (ppm)	Partition coefficient	Sensitivity (10^{-3} %RH/Hz)	Resolution (10^{-3} %RH)	Partition coefficient
APTMS/PTMS	2.02	14.1[a]	28	25	1.61	3.25	54
APTES	0.38	1.66	0.63	175	1.16	0.44	62
Homo-polyimide	0.41	57.8	24	8	0.96	0.39	115
Guanidine	4.62	0.75[b]	3.5[b]	471	0.18	0.83	484
		1.06[c]	4.9[c]				
		3.84[d]	17.7[d]				

[a] 60 °C.
[b] Before saturation.
[c] After regeneration.
[d] In air.

0–1.2%) to estimate the volume sensitivity. Among the four functionalization layers, guanidine shows the highest sensitivity to CO_2 concentration (Table 3).

In addition, we computed a partition coefficient, *K*, for each layer for a performance comparison to include the effect of different thicknesses of the functionalization layers. *K* is defined as a ratio between concentration in the stationary phase, *Cs* (absorbed in the functionalization layer) and concentration in the vapor phase, *Cv* [15]:

$$K = \frac{\delta Cs}{\delta Cv} = \left(\frac{1}{S \times \rho \times A \times t_p}\right)\left(\frac{\Delta m}{\Delta f_0}\right),$$

where *S* is the volume sensitivity in Hz^{-1}, ρ is the gas concentration in kg/m^3, *A* is the detection area in cm^2, t_p is the thickness of the polymer in cm, and $\Delta m/\Delta f_0$ is the device mass sensitivity in g/kHz. Guanidine also shows the highest partition coefficients to CO_2 compared to other layers.

3.2. Guanidine polymer

3.2.1. Polymer saturation and regeneration

The CMUT functionalized with the guanidine polymer exhibited the largest response to CO_2 at ambient condition, and, thus, is the recommended polymer for further experiments. We have investigated this polymer in terms of polymer saturation, regeneration, and repeatability – all important characteristics for implementing a practical CO_2 sensor.

We observed that the volume sensitivity of the guanidine-coated sensor worsened over time when exposed to a CO_2 concentration above 16,000 ppm (i.e. 1.6%). Specifically, at each cycle, the sensor was exposed to 2-min pulses of CO_2 concentrations from 0 ppm to 20,000 ppm in an increment of 4000 ppm. The sensor was exposed to three consecutive cycles and the volume sensitivity degraded at each cycle (Fig. 6). After these three cycles, the polymer was regenerated (i.e. a process to restore the absorptive capacity by desorbing adsorbed analytes) and the sensor was exposed to another three consecutive cycles. The sensitivity estimated from the first cycle after regeneration indicated that the polymer regeneration was successful in recovering the sensitivity. However, exposing the sensor to a CO_2 concentration above 16,000 ppm again resulted in a similar degradation in the volume sensitivity (Fig. 6).

A possible cause for this degradation in the sensitivity is semi-permanent saturation of the polymer where the absorbed CO_2 is not fully removed through the standard purging with N_2. This semi-permanent saturation might be due to presence of a second reaction between CO_2 and a sorption site that is different from the primary sorption site. If this second reaction requires higher activation energy for absorption and desorption than that of the primary reaction, the amount of absorbed CO_2 from the second reaction will become significant at high CO_2 concentrations. Because higher activation energy is required to remove this absorbed CO_2, the standard purging might not be sufficient. The residual CO_2 would then result in the semi-permanent saturation of the polymer. One way to regenerate the polymer to reverse the semi-permanent saturation is to provide a higher energy to facilitate the reverse reaction to occur by increasing the temperature. We regenerated the polymer by heating the guanidine-coated sensor to 120 °C at a rate of 10 °C/min and then holding the temperature at 120 °C for 20 min. The polymer was saturated and regenerated twice to examine the robustness of the regeneration procedure. The volume sensitivities of the first cycles after two regenerations are comparable to each other (Fig. 7).

The challenge with using the guanidine polymer is the need for polymer regeneration when the layer is exposed to a CO_2 concentration above 16,000 ppm. For environmental monitoring applications, we can design the sensor to alarm when the concentration increases above the TLV of 5000 ppm to prevent polymer saturation. If the sensor system must be designed to withstand the exposure to CO_2 concentration above 16,000 ppm, an electrical heating wire can be implemented underneath the sensor to perform the polymer regeneration.

In the last cycle, the volume sensitivity of 1.06 ppm/Hz was measured by exposing the sensor to even a lower range of

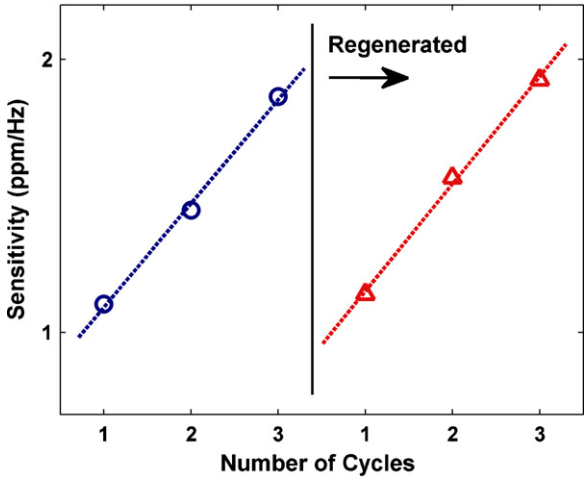

Fig. 6. Plot of volume sensitivity to CO_2 calculated from each cycle of exposing the sensor to 2-min CO_2 pulses from 0 ppm to 20,000 ppm in an increment of 4000 ppm, in N_2. After three initial cycles, the polymer was regenerated and additional three consecutive cycles were applied.

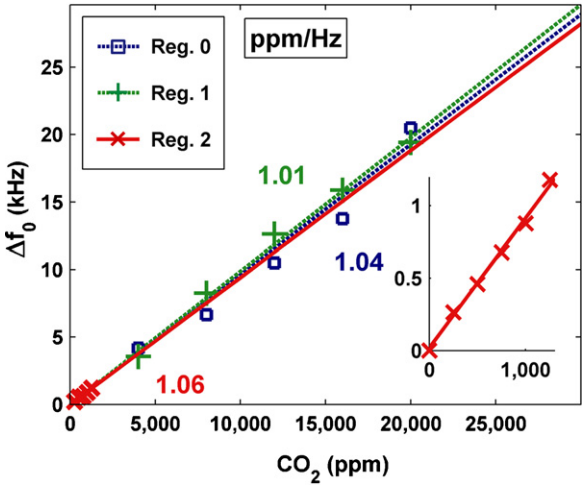

Fig. 7. Plot of maximum frequency shifts observed at different CO_2 concentrations in N_2 at the first cycle of each regeneration. The inset shows the maximum frequency shifts of the guanidine sensor exposed to a lower range of concentrations from 0 ppm to 1250 ppm demonstrating a distinguishable pulse as low as 250 ppm.

concentration from 0 to 1250 ppm with an increment of 250 ppm (Fig. 7 (inset)). The lower concentrations were generated by using a mass flow controller with a larger flow capacity. The sensor exhibited a distinguishable frequency shift (~52 times the noise floor) to CO_2 concentration of 250 ppm, which is smaller than the ambient CO_2 concentration of 300 ppm. In addition, the sensor was exposed to CO_2 in air (~45%RH) instead of in N_2 (Fig. 8). While the sensitivity has decreased by three times due to the presence of water in air (3.84 ppm/Hz), the sensor sensitivity and resolution are more than sufficient to be used at ambient condition.

3.2.2. Sensor repeatability

We evaluated the repeatability of the sensor system by exposing the sensor to 19 consecutive pulses of 4000 ppm of CO_2 over a time period of 2.5 h. At each cycle, the sensor was exposed to 4000 ppm of CO_2 for 120 s and then purged with N_2 for the next 240 s. The sensor successfully responded to every pulse of CO_2 without degradation in sensitivity with a mean frequency shift of 4.75 kHz and a standard deviation of 256 Hz (Fig. 9).

3.2.3. Cross-sensitivity to water vapor

A common problem with functionalization layers, sensitive to CO_2, is their high responses to water vapor, as H_2O is often required in the chemical reaction. Thus, we exposed the CMUT to various concentrations of H_2O in dry N_2 from 0%RH to 80%RH. As expected, the four functionalization layers exhibited high sensitivities to relative humidity, and the layers with higher volume sensitivities to CO_2 also exhibited higher sensitivities to H_2O (Fig. 10). Potential solutions to the high cross-sensitivities to water vapor include

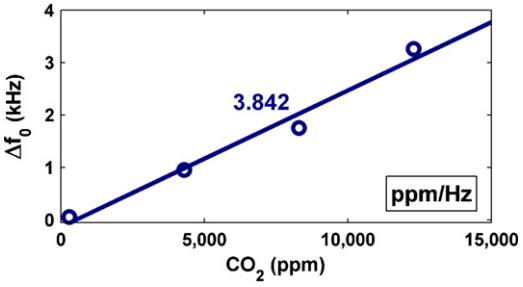

Fig. 8. Plot of maximum frequency shifts observed at different CO_2 concentrations in air (~45%RH).

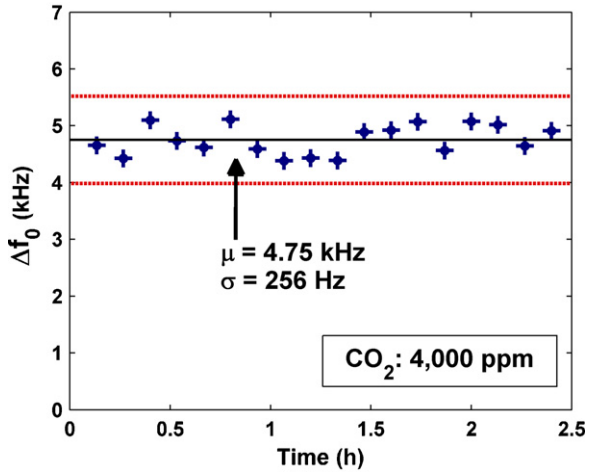

Fig. 9. Plot of maximum frequency shifts to 18 pulses of 4000 ppm CO_2 concentration over 2.5 h showing the mean (black line) and $\pm 3\sigma$ (dotted line) frequency shifts.

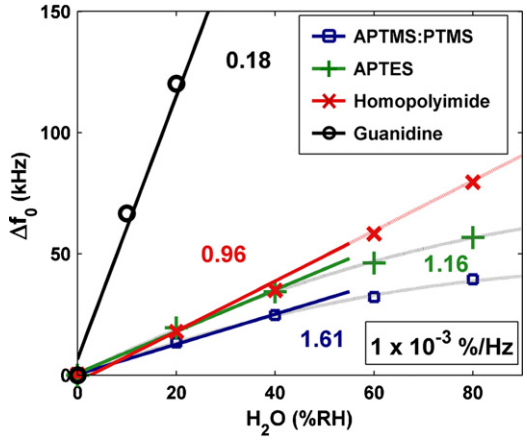

Fig. 10. Plot of maximum frequency shifts observed at different H_2O concentrations for four sensors and linear fits to estimate the volume sensitivities.

using a reference sensor that is either not exposed to humidity or is sensitive only to humidity. Another solution is using array implementations with different sensitive layers to perform pattern recognition [4].

4. Conclusion

This paper has presented a comparative study of four functionalization layers, including polymers functionalized with basic, amine-bearing functional groups and a polyimide with high solubility, for CO_2 detection using a 50-MHz CMUT as highly sensitive resonant sensor platform. We demonstrated through the comparative study that the guanidine polymer is a promising functionalization layer for CO_2 detection, which exhibited an excellent sensitivity of 1.06 ppm/Hz and a resolution of 4.9 ppm to CO_2 in ambient condition. The presented sensor has more than sufficient sensitivity and resolution to track CO_2 concentration in ambient condition. In addition, by presenting other characteristics including polymer regeneration, sensor repeatability, and cross-sensitivity to water vapor, we have addressed practical issues of using guanidine polymer as a functionalization layer for CO_2 detection.

Acknowledgements

We thank Defense Advanced Research Projects Agency, Microsystems Technology Office for their financial support of this project through grant N66001-06-1-2030. We would like to also thank Ira Wygant and Wei Ma at National Semiconductor, Santa Clara, CA, Matthias Steiert at Matrix Sensors Inc., Pleasanton, CA, and Christine Cuppoletti at Stanford Research Institute, Menlo Park, CA, for financial support, polymer coating, and guidance.

References

[1] N.V. Kirianaki, S.Y. Yurish, N.O. Shpak, V.P. Deynega, Data Acquisition and Signal Processing for Smart Sensors, 1st ed., Wiley, New York, 2002.
[2] M. Li, E.B. Myrs, H.X. Tang, S.J. Aldridge, H.C. McCaig, J.H. Whiting, R.J. Simonson, N.S. Lewis, M.L. Roukes, Nanoelectromechanical resonator arrays for ultrafast, gas-phase chromatographic chemical analysis, Nano Letters 10 (10) (2010) 3899–3903.
[3] R. Zhou, D. Schmeisser, W. Gopel, Mass sensitive detection of carbon dioxide by amino group-functionalized polymers, Sensors and Actuators B: Chemical 33 (1996) 188–193.
[4] A.E. Hoyt, A.J. Ricco, J.W. Bartholomew, G.C. Osbourn, SAW sensors for the room-temperature measurement of CO_2 and relative humidity, Analytical Chemistry 70 (1998) 2137–2145.
[5] H.J. Lee, K.K. Park, M. Kupnik, Ö. Oralkan, B.T. Khuri-Yakub, Chemical vapor detection using a capacitive micromachined ultrasonic transducer, Analytical Chemistry 83 (2011) 9314–9320.
[6] G. Sberveglieri, Recent developments in semiconducting thin-film gas sensors, Sensors and Actuators B: Chemical 23 (1995) 103–109.
[7] H.J. Lee, K.K. Park, M. Kupnik, N.A. Melosh, B.T. Khuri-Yakub, Mesoporous thin-film on highly-sensitive resonant chemical sensor for relative humidity and CO_2 detection, Analytical Chemistry 84 (2012) 3063–3066.
[8] S. Sivaramakrishnan, R. Rajamani, C.S. Smith, K.A. McGee, K.R. Mann, N. Yamashita, Carbon nanotube-coated surface acoustic wave sensor for carbon dioxide sensing, Sensors and Actuators B: Chemical 132 (2008) 296–304.
[9] J.R. Vig, Kim Yoonkee, Noise in microelectromechanical system resonators, IEEE Transactions on Ultrasonics, Ferroelectrics and Frequency Control 46 (1999) 1558–1565.
[10] K.K. Park, H.J. Lee, M. Kupnik, B.T. Khuri-yakub, Fabrication of capacitive micromachined ultrasonic transducers via local oxidation and direct wafer bonding, Journal of Microelectromechanical Systems 20 (2011) 95–103.
[11] L. Meirovitch, Analytical Methods in Vibrations, 1st ed., Macmillan, New York, 1967.
[12] S. Sherrit, H.D. Wiederick, B.K. Mukherjee, Accurate equivalent circuits for unloaded piezoelectric resonators, IEEE Ultrasonics Symposium, IEEE (1997) 931–935.
[13] A. Brandenburg, R. Edelhaäuser, Integrated optical gas sensors using organically modified silicates as sensitive films, Sensors and Actuators B: Chemical 11 (1993) 361–374.
[14] D.W. Allan, Time and frequency (time-domain) characterization, estimation, and prediction of precision clocks and oscillators, IEEE Transactions on Ultrasonics, Ferroelectrics and Frequency Control 34 (1987) 647–654.
[15] J.W. Grate, A. Snow, D.S. Ballantine, H. Wohltjen, M.H. Abraham, R.A. McGill, P. Sasson, Determination of partition coefficients from surface acoustic wave vapor sensor responses and correlation with gas–liquid chromatographic partition coefficients, Analytical Chemistry 60 (1988) 869–875.

Biographies

Hyunjoo Lee (S'04) received the B.S. degree in electrical engineering and computer science and the M.Eng. degree in electrical engineering from the Massachusetts Institute of Technology, Cambridge, in 2004 and 2005, respectively. She is currently working toward the Ph.D. degree in electrical engineering at Stanford University, Stanford, CA, expected to graduate in September 2012. From 2004 to 2005, she was an MIT VI-A Fellow at Analog Devices, Inc., Wilmington, MA, where she studied continuous-time signal-delta ADCs. From 2008 to 2011, she was an Engineering Intern at National Semiconductor, Santa Clara, CA (now, TI Silicon Valley Labs, Texas Instrument) where she developed an oscillator circuit that interfaces with a capacitive micromachined ultrasonic transducer (CMUT) for chemical sensing. Her research interests include sensor interface circuit design and bio/chemical sensor design. She is also a member of the Eta Kappa Nu and Tau Beta Pi honor societies.

Kwan Kyu Park (S'08) received the B.S. degree in mechanical and aerospace engineering from Seoul National University, Seoul, Korea, in 2001. He received the M.S. degree and the Ph.D. degree in mechanical engineering from Stanford University, Stanford, CA, in 2007 and 2011. He was a Research Assistant in the Edward L. Ginzton Laboratory, Stanford University, since 2006 until 2011, and is currently working as a Postdoctoral Researcher in Prof. Khuri-Yakub's group at Stanford University since 2011. His research interests include chemical/bio sensors based on micromechanical resonators, multiresonator systems, charging of MEMS devices, ultrasonic transducers, and RF MEMS. He is currently working on ultrasonic imaging systems based on micromachined ultrasonic transducers (CMUTs).

Mario Kupnik (SM'09) received the Diplom Ingenieur degree from the Graz University of Technology, Graz, Austria, in 2000, and the Ph.D. degree from the University of Leoben, Leoben, Austria, in 2004. He is currently working as a Professor of electrical engineering with the Brandenburg University of Technology, Cottbus, Germany. Since 2005, he has been a Postdoctoral Researcher, Research Associate, and Senior Research Scientist with the group from Prof. Khuri-Yakub at the Edward L. Ginzton Laboratory, Stanford University, Stanford, CA, until 2011. Before his Ph.D. studies (2000–2004), he was with Infineon Technologies AG, Graz, working as an Analog Design Engineer in the field of ferroelectric memories and contactless smart card systems. He has authored and coauthored more than 70 publications and has been the Principal Inventor and Coinventor of ten U.S. and international issued patents, relating to analog front-end circuits for contactless smart card systems, ultrasonic transit-time gas flowmeters, capacitive micromachined ultrasonic transducers fabrication techniques and modeling, high-temperature ultrasound transducers, and bio/chemical sensors. Dr. Kupnik was the recipient of several research awards for his doctoral thesis, e.g. the 2004 Fred–Margulies Award of the International Federation of Automatic Control. Since 2007, he has served on the technical program committee of the IEEE Ultrasonics Symposium.

Butrus T. Khuri-Yakub (F'95) received the B.S. degree in electrical engineering from the American University of Beirut, Beirut, Lebanon, the M.S. degree in electrical engineering from Dartmouth College, Hanover, NH, and the Ph.D. degree in electrical engineering from Stanford University, Stanford, CA. He is a Professor of electrical engineering at Stanford University. His current research interests include medical ultrasound imaging and therapy, chemical/biological sensors, micromachined ultrasonic transducers, and ultrasonic fluid ejectors. He has authored over 500 publications and has been the principal inventor or coinventor of 88 U.S. and international issued patents. Dr. Khuri-Yakub was the recipient of the Medal of the City of Bordeaux in 1983 for his contributions to nondestructive evaluation, the Distinguished Advisor Award of the School of Engineering of Stanford University in 1987, the Distinguished Lecturer Award of the IEEE Ultrasonics, Ferroelectrics, and Frequency Control Society in 1999, a Stanford University Outstanding Inventor Award in 2004, and a Distinguished Alumnus Award of the School of Engineering of the American University of Beirut, in 2005.